Multilayer Technology of Decorated Plasters from the domus of Marcus Vipsanus Primigenius at Abellinum (Campania Region, Southern Italy): An Analytical Approach

Sabrina Pagano, Chiara Germinario, Maria Francesca Alberghina, Marina Covolan, Mariano Mercurio, Daniela Musmeci, Rebecca Piovesan, Alfonso Santoriello, Salvatore Schiavone, Celestino Grifa

minerals

MDPI

Article

Multilayer Technology of Decorated Plasters from the *domus* of *Marcus Vipsanus Primigenius* at *Abellinum* (*Campania* Region, Southern Italy): An Analytical Approach

Sabrina Pagano [1], Chiara Germinario [1,2,*], Maria Francesca Alberghina [3,4], Marina Covolan [5,6], Mariano Mercurio [1,2], Daniela Musmeci [5], Rebecca Piovesan [7], Alfonso Santoriello [5], Salvatore Schiavone [4] and Celestino Grifa [1,2]

1 Department of Science and Technology, University of Sannio, 82100 Benevento, Italy
2 CRACS—Center for Research on Archaeometry and Conservation Science, 80126 Napoli, Italy
3 Department of Biology, Ecology and Earth Science (DiBEST), University of Calabria, 87036 Arcavacata di Rende, Italy
4 S.T.Art-Test di S. Schiavone & C. sas, 93015 Niscemi, Italy
5 Department of Cultural Heritage, University of Salerno, 84084 Fisciano, Italy
6 Centre Jean Bérard, UAR3133, CNRS-EFR, Via Francesco Crispi, 86, 80121 Napoli, Italy
7 LAMA—Laboratory for the Analysis of Ancient Materials, University Iuav of Venice, Calle Della Laca, San Polo 2468, 30125 Venice, Italy
* Correspondence: chiara.germinario@unisannio.it

Abstract: Situated on the left bank of the *Sabato* river, the city of *Abellinum* (*Campania* region, southern Italy) represents a tangible testimony to the influence of the Roman civilization in *Irpinia*. At the site, where the remains of the public area of the town are preserved, archaeological excavations unearthed a monumental Pompeian *domus*, likely owned by *Marcus Vipsanius Primigenius*, a freedman of *Agrippa*, son-in-law of *Augustus*. The rooms preserved fine wall paintings of 3rd and 4th Pompeian style, reflecting the social status of the owner. From four rooms overlooking the peristyle, eight specimens of decorated plasters were collected, and petrographic and spectroscopic analyses were carried out to investigate the plastering and painting technology. Thin sections of all plasters depicted a multilayer technology, although differences in mix designs of the supports were highlighted. Some samples are pozzolanic plasters, containing volcanic aggregate, others can be classified as *cocciopesto* because of the presence of ceramic fragments mixed to the volcanic aggregate. Finally, the presence of marble powder also permitted the identification of *marmorino*. Moreover, the pigments, applied using *a fresco* or lime-painting techniques, consist of pure or mixed Fe- and Cu-based pigments to obtain yellow, orange, red, pink, and blue decorations.

Keywords: plasters; multilayer technology; *cocciopesto*; *marmorino*; pigments; spectroscopy; Roman epoch; *Abellinum*

Citation: Pagano, S.; Germinario, C.; Alberghina, M.F.; Covolan, M.; Mercurio, M.; Musmeci, D.; Piovesan, R.; Santoriello, A.; Schiavone, S.; Grifa, C. Multilayer Technology of Decorated Plasters from the *domus* of *Marcus Vipsanus Primigenius* at *Abellinum* (*Campania* Region, Southern Italy): An Analytical Approach. *Minerals* **2022**, *12*, 1487. https://doi.org/10.3390/min12121487

Academic Editor: Daniele Moro

Received: 8 November 2022
Accepted: 20 November 2022
Published: 23 November 2022

1. Introduction

Decorated plasters have great importance among the various archaeological finds studied with a multi-analytical approach. The main reason lies in the high number of well-preserved buildings, especially in volcanic areas of *Campania* region. *Pompeii* and *Herculaneum*, in particular, represent outstanding examples of still preserved ancient cities "frozen" by eruptions, which offer a great contribution to understanding how ancient Romans built their houses and decorated their rooms [1–3]. In recent years, the research highlighted many of the constructive and pictorial characteristics used by the ancient Roman masters, including contexts outside the well-known archaeological parks. The studies carried out to investigate decorated plasters revealed the accurate multilayer technologies made with different recipes of binders and aggregates. Such diversity led to thin plaster layers with specific technical features being obtained. In particular, natural and/or artificial

aggregates were used; peculiar is the use of coarse-grained ceramic fragments or *pozzolana* to improve the hydraulicity of the mortars, as well as the use of marble powder to assure specific waterproofing characteristics [1,4,5]. The various layers were often completed with a surface finish layer that hosted the paint, by diversified colour application techniques (e.g., *fresco*, *secco*) [2,6,7]. These examples were observed also in the innermost territory of the *Campania* region, which corresponds to the modern *Avellino* province, called *Irpinia*, from the ancient Samnite tribes that occupied this area, named *Hirpini* (from latin *Hirpus*, wolf). High mountains and smooth hills are features of the typical landscape of this Southern Apenninic land, often crossed by river valleys which represented the easiest paths for human connections. The historical evolution of this vast territory (ca. 3000 km^2) has always been influenced by this articulated landscape since the Apennine chain offered few natural trajectories from W to E, along which cultural centres arose. For example, in the NE portion of this region (Higher *Irpinia*) two important Roman roads passed, the *Appia* and *Traiana* roads, giving birth to crucial settlements in the transit to eastern territories, such as *Aeclanum*. Meanwhile, the SW part of this region (Lower *Irpinia*) had an important role in connecting the inner territories with the Southern coast of Salerno, and the junction between *Appia* and *Capua-Rhegium* roads was made possible by the *Sabato* river (Figure 1a).

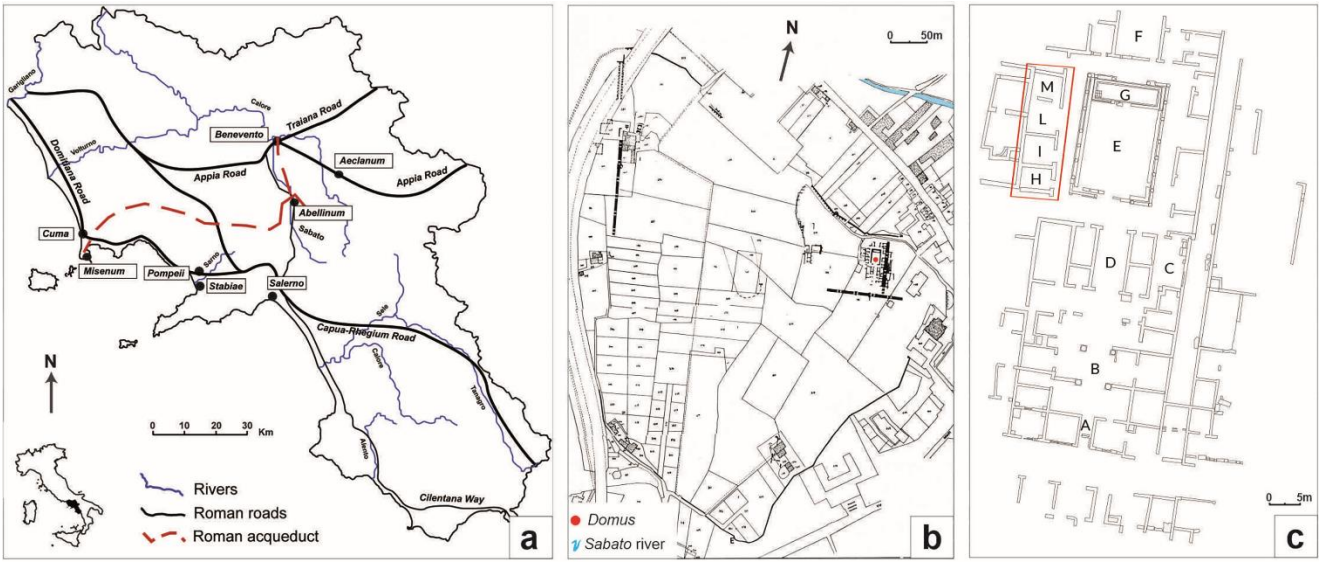

Figure 1. (**a**) Sketch map of *Campania* region, with the location of the ancient city of *Abellinum* (modified from [8]); (**b**) Map of the ancient city of *Abellinum* where the *domus* was unearthed (modified from [9]); (**c**) Plan of the *domus* (investigated rooms are reported in the red box).

On the left side of this river, the *Hirpini* founded a settlement named *Abellinum*, in the modern town of *Atripalda* [9]. Framed in the 3rd–4th century BCE, this first settlement exploited the advantages of the top of a large tuff dome referable to the Campanian Ignimbrite eruption [10]. The dome offered a large view of the territory along with a position conducive to protection and the availability of natural building resources (stones and volcanic sands).

Abellinum participated in Samnitic wars up to the romanisation of the town in the Sillan age.

The city became a flourishing centre with several public and private buildings and it was included in *Regio I* by *Emperor Augustus* (*Latium et Campania*) [11,12]. During the Late Republican age, *Abellinum* knew its period of maximum expansion; the ancient settlement was 250.000 m^2 large and was protected by 2 km of walls made of *opus reticulatum* with doors that opened towards the NE (*Aeclanum*) and SW (*Salerno*) and several circular towers. The settlement was organised in several blocks of private buildings surrounded by an

EW-directed paved *decumanus* and several secondary orthogonal roads; the presence of a thermal edifice and the forum highlighted a vivid social activity.

Among the private edifices stands out a large Pompeian-type *domus* with peristyle and *atrium* built in a favourable view towards the valley (Figure 1b). Considering the architecture and the quality of internal decorations, the owner is believed to have belonged to the highest ranks of the local elite [9,13].

Other remains proved the occurrence of significant monuments such as the amphitheatre outside the wall; however, probably the most important infrastructure in the *Abellinum* territory is the still active *Fontis Augustei Aquaeductus*. It is articulated in different branches, one of which provided water in the *territorium neapolitanum* up to *Capo Miseno* (Phlegraean Fields, Naples), while the other branch reached the *Beneventum* town [9,14].

Like most territories of the Roman Empire, even *Abellinum* suffered the social and economic crises of the Late Roman period, aggravated by two main natural events: an earthquake in 346 CE and the *Pollena* eruption in 472 CE, which caused a slow abandonment of the hill towards new territories where the modern *Avellino* is located [13].

The archaeological patrimony of this part of the *Campania* region has been the object of spotted surveys and research by scholars and officers of the local superintendence, far from the interest of the most attractive archaeological sites along the cost (*Cumae, Puteoli, Pompeii, Herculaneum, Paestum*). Generally, monumental heritage and scattered settlement, as well as necropolis and sanctuary [9], are often investigated as emergency works and preventive archaeological interventions. The identification and cataloguing of objects are the archaeological tools capable of unveiling the material culture of this ancient population.

The project (*Abellinum. Piano per la conoscenza, la tutela e la valorizzazione dell'antico centro irpino*), headed by the Department of Heritage Science of the University of Salerno, was launched in 2019 in synergy with the *Soprintendenza Archeologia, Belle Arti e Paesaggio* for the Provinces of *Salerno* and *Avellino* and the Municipality of *Atripalda*, in order to achieve, on one side, the promotion of programs for the protection, enhancement, and redevelopment of the archaeological area and, on the other, the extension of the archaeological, dynamic map of the ancient *Abellinum*, allowing the important historical-archaeological issues that are still open and little known to be addressed.

The collaboration of the Department of Science and Technology of the University of Sannio in this project attains to unveil the peculiar aspects of material culture, and the present paper deals with the investigation of decorated plasters collected in the *domus* in order to shed light on the different material resources adopted for the manufacture of plaster, along with the types of pigment and painting techniques used by the skilled workers and artists. To this scope, a multi-analytical approach was adopted, based on the implementation of spectroscopic techniques on the surfaces of decorated plasterm and optical and electron microscopy coupled with energy dispersive X-ray spectroscopy on stratigraphic thin sections.

2. The Archaeological Context

The *domus* is by far the most impressive building of the settlement; it occupies an entire block with the entrance just on the *decumanus*. The property was attributed to *Marcus Vipsanus Primigenius*, a freedman of *Vipsanius Agrippa* (son-in-law of *Augustus*), following the inscription on a bronze seal dated back to the early Imperial period [13,14].

This patrician house had at least four building and occupation phases as highlighted by archaeological surveys; in its largest occupation (from the middle of the 1st century BCE to 3rd-4th century CE), the *domus* reflects the room divisions and functions in a Roman house (Figure 1c). The southern part was occupied by the vestibule (A) and the tetrastyle *atrium* (B), surrounded by representative and service areas, such as the kitchen (C) in the north-eastern corner (Figure 1c). The *tablinum* (D) divides this first sector from the peristyle area (E) with the rooms around it, built later than the first portion of the *domus* (Figure 1c). A series of living rooms opened towards the north to the view on the valley, and all the

representative rooms were decorated with wall paintings in 3rd and 4th Pompeian style with floral and garland motifs or with the imitation of precious marbles (Figure 2a–c) [13].

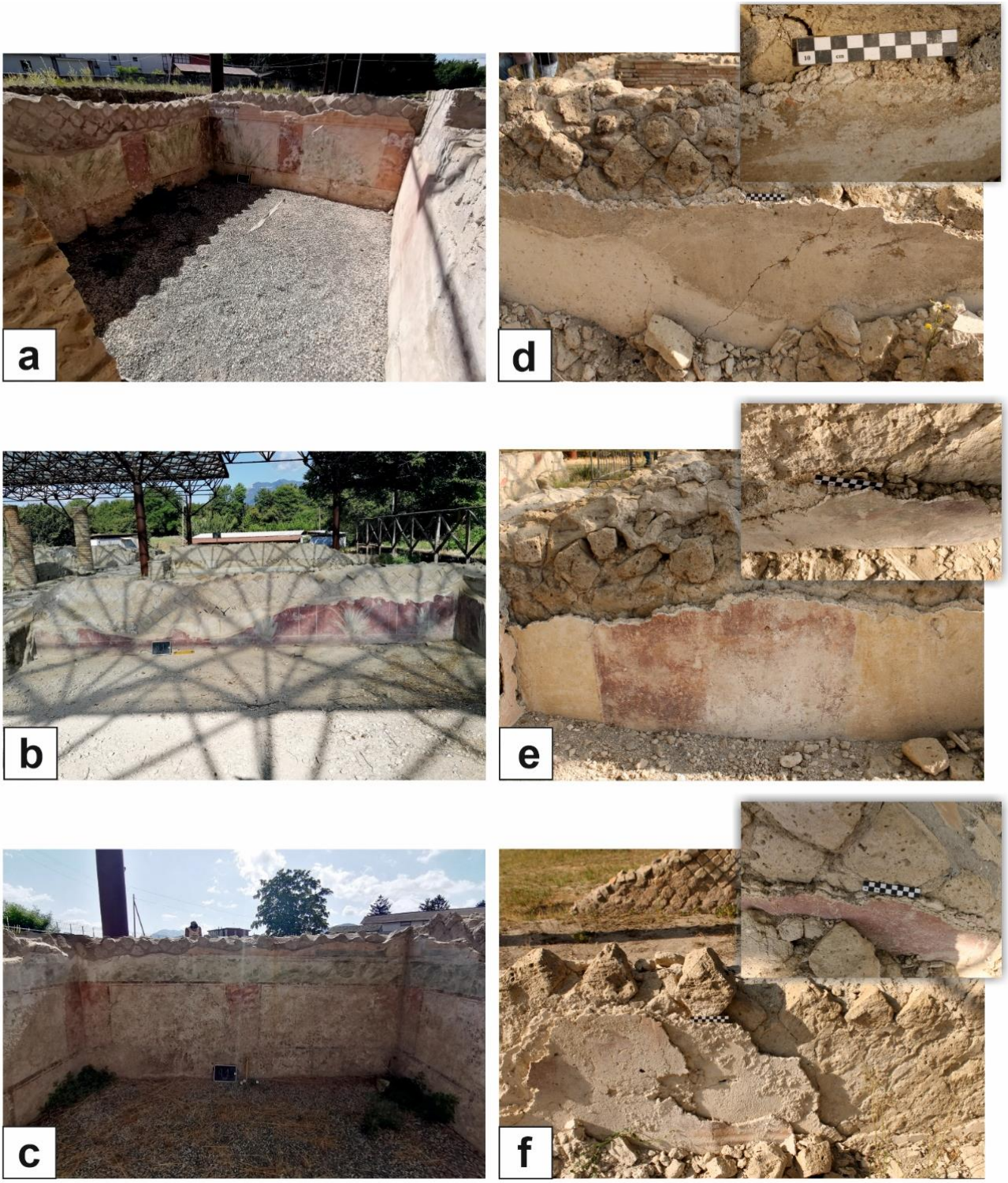

Figure 2. Rooms of the *domus* decorated with floral motifs (**a**,**b**) and imitation of precious marbles and stones (**c**); plaster of room I (**d**) containing ceramic fragments (inset in (**d**)); plaster of room L (**e**) on which the pictorial layer is still preserved (inset in (**e**)); plasters of room M (**f**), characterised by an inner layer of mortar containing ceramic fragments, on which an outer decorated plaster's layer was applied (inset in (**f**)).

The decorative apparatus reflects the high level of both patronage and workmanship, especially when also considering the floor of the central *oecus* (F) made in *opus sectile* with polychrome stones and geometrical motifs. The square plan peristyle was surrounded by a portico with columns (Figure 2b) covered with red coloured plasters and hosted a *natatio* (a pool; G) for the *otium* of the owners. On the western side, other living rooms opened to the peristyle (Figure 1c; H, I, L, M). They still preserve traces of the pictorial decoration, although the collapsed wall structures have deeply disaggregated the plaster and only a few signs of wall paintings have survived so far (Figure 2d–f). However, the collapses highlighted the original structures of the plasters, occasionally featuring a complex stratigraphy, showing two superimposed interventions in some rooms (Figure 2f). Rooms I, L and M appear to have undergone several interventions, due in part to some repairs or reconstructions that were carried out following structural damage (probably caused by an earthquake), but also determined by the addition of the rooms to the west of those under examination, attributable to the construction of a complex—possibly for bath and thermal use. A better chronological sequence and a more accurate functional definition will be verified in future research. In rooms H, I, L, and M, we collected the decorated plaster for analytical investigation. The *domus* was only partially restored and reused after the 472 CE eruption, mostly in the southern sector where the older vestibule and the tetrastyle *atrium* were located.

3. Samples and Analytical Techniques

For this study, eight multi-layered plasters (AB1-8) from four living rooms located west of the peristyle were investigated (Table 1, Figure 1c). In particular, the sample AB1 was collected in the H room, AB2 in the I room (Figure 2d), AB3 and AB4 came from the L room (Figure 2e), and, finally, AB5, AB6, AB7, and AB8 were sampled in M room (Figure 2f), where two superimposed layers of plasters were observed (Table 1). In particular, samples AB5 and AB8 were collected from the inner layer, whereas AB6 and AB7 are referred to the outer layer (Figure 2f; Table 1).

Table 1. Macroscopic features of multi-layered plasters.

Sample	Room	Layer	Colour	Approximate Size (L × l) (cm)	Thickness (cm)	Cohesion	Lumps
AB1	H	*Arriccio* *Intonachino* Pictorial layer	White White White/Red	3.8 × 1.5	≥0.9 ca. 0.5 <0.1	Cohesive Cohesive -	Rare Rare -
AB2	I	*Arriccio* *Intonachino* Finishing	Light grey White White	4.2 × 2.2	≥1.1 ca. 0.7 <0.1	Friable Friable -	Frequent Rare -
AB3	L	*Arriccio* *Intonachino* Pictorial layer	Orange-grey White Red/Yellow/Orange	6.0 × 3.0	≥1.5 ca. 0.4 <0.1	Friable Friable -	Frequent Frequent -
AB4	L	*Arriccio* *Intonachino* Pictorial layer	Light grey White Pink/Blue	4.0 × 2.4	≥1.7 ca. 0.2 <0.1	Friable Cohesive -	Frequent Rare -
AB5	M	*Arriccio* *Intonachino* Finishing	Pinkish-grey White White	4.5 × 3.0	≥0.8 ca. 0.4 <0.1	Friable Friable -	Frequent Frequent -
AB6	M	*Arriccio* *Intonachino* Pictorial layer	Light grey White Pink/Light blue	4.2 × 2.2	≥0.7 ca. 1.0 ca. 0.2	Friable Cohesive -	Rare Rare -
AB7	M	*Arriccio* *Intonachino* Pictorial layer	Light grey White Red	3.6 × 3.0	≥1.0 ca. 0.6 <0.1	Friable Friable -	Rare Rare -

Table 1. *Cont.*

Sample	Room	Layer	Colour	Approximate Size (L × l) (cm)	Thickness (cm)	Cohesion	Lumps
AB8	M	*Arriccio*	Pinkish-grey	3.0 × 2.0	≥1.2	Friable	Frequent
		Intonachino	White		ca. 0.4	Friable	Rare
		Finishing	White		<0.1	-	-

Legend: L, major side; l, minor side. The approximate size is referred to the entire fragment.

The sampling of both plaster layers was carried out in order to highlight the similarities or differences between the two different building phases. These rooms, in fact, clearly show two moments in the *domus*' life through the rough superimposition of two plasters likely due to (i) the reorganisation of the internal spaces and their new destination of use or (ii) the restoration works after damages probably caused by one of the earthquakes that affected the city of *Abellinum* during the Roman Imperial period.

While only a white finishing surface was observed on the samples AB2, AB5, and AB8, samples AB1, AB3, AB4, AB6, and AB7 preserved a coloured painting layer, used to finish the surface of walls.

The analytical strategy adopted provided for a multi-analytical approach, based on the combined use of spectroscopic techniques on pictorial layers, and microscopy on mortar-based supports.

The pictorial layers were first explored via digital microscopy using a Dino-lite digital microscope with a magnification range of 400x–470x, built-in coaxial illumination and Flexible LED Control (FLC), equipped with a 5.0-megapixel colour CMOS sensor. Images have been acquired by DinoCapture2.0 software. Then, when possible, spectrophotometric analyses were performed by Fiber Optics Reflectance Spectroscopy (FORS) in the spectral range 380–1050 nm by using a tungsten lamp (BeWTek, Inc., San Antonio, TX, USA) BPS101 Tungsten Halogen Light Source with a spectral range of 350 to 2600nm) as source and the grating Qmini Broadcom as detector. The measuring head geometry was 45°/0°. A B&WTek inc. white plate (99%) was used as a reference. To obtain the colorimetric coordinates the primary illuminant D65 and the standard observer CIE 10° (CIE 1964) were set. The analysed area was 2 mm^2 and each acquired spectrum was the average of 128 scans (measurement time 0.04 s). For each sample, three measurements were carried out.

Elemental chemical composition of the pictorial layers was determined by M1 MISTRAL Bruker XRF spectrometer (50 kV/800 μA power supply, collimator size 0.5 × 0.5 mm, silicon drift SDD detector). Molecular composition for the identification of main mineralogical phases was obtained by BRUKER Alpha FTIR spectrometer using an Attenuated Total Reflectance (ATR) module; absorption spectra were collected in a spectral range between 4000 and 400 cm^{-1} with a diamond crystal, at the resolution 4 cm^{-1}, with 64 scans performed for each run.

Plasters were first photographed and described from the macroscopic point of view according to the UNI-EN 11305: 2009 and UNI-EN 11176: 2006 standards [15,16]. Then, mineralogical composition and textural features were determined by Polarized Light Microscopy (PLM) on stratigraphic thin sections (ca. 30 μm) by using a Nikon Eclipse 6400 POL microscope equipped with a Nikon DS-Fi camera. To determine the Grain Size Distribution (hereafter GSD) we used microphotographs (both in plane- and cross-polarized light) analysed by Digital Image Analyses (DIA). The minimum Feret (mF) values were measured by ImageJ software and its value was used to calculate Krumbein φ (where $\varphi = -\log_2(\text{mF})$). To avoid the overestimation of binder that DIA could determine, abundance of aggregate and the estimation of binder-to-aggregate ratio (B/A) was obtained by visual estimation [17]. The software Bruker Opus 7.2 was adopted also for data acquisition and processing. The determination of the hydraulic properties of the binder was carried out on carbon-coated thin sections by Scanning Electron Microscopy (SEM) with a Zeiss EVO 15 HD VPSEM operating at 20 kV accelerating voltage, coupled with Oxford Instruments

Microanalysis Unit with Xmax 80 EDS detector. Standards details used for EDS calibrations are reported in by Germinario and co-authors [18].

4. Results

4.1. Supports

All samples collected from the walls of the *domus* consist of a multi-layered plasters formed by three layers. Macroscopic observation revealed three different mix-designs used for making plasters. In particular, samples AB2 (room I; Figure 2d), AB5, and AB8 (inner plaster's layers of room M; Figure 2f) are featured by the presence of ceramic fragments as aggregate (*cocciopesto*), samples AB1, AB3, and AB4 contain volcanic aggregate (pozzolanic plasters), and samples AB6 and AB7 are marked by the presence of marble dust (*marmorino*) (Table 2).

Table 2. Mineralogical and textural features of analysed plasters, obtained by means of PLM and DIA.

Sample	Layer	Binder Features	Mineralogy of Aggregate	Aggregate (%)	B/A	GSD (mm)			
						Max	Min	av. φ_{mF}	S (φ_{mF})
AB1	*Arriccio*	Crypt., Anisotr.	Pum, Sc, Cpx, Afs, Qz ^{tr}	20	4.0	0.87	0.02	2.5	1.16
	Intonachino	Crypt., Anisotr.	Cal, CF	20	4.0	0.99	0.05	2.2	1.08
AB2	*Arriccio*	Micr., Anisotr.	Pum, Sc, Cpx, Afs, Cer, Ol ^{tr}, Qz ^{tr}	30	2.3	1.49	0.06	1.7	0.91
	Intonachino	Micr., Anisotr.	Pum, Sc, Cer, Cpx, Afs	30	2.3	1.86	0.04	2.6	1.12
AB3	*Arriccio*	Micr., Anisotr.	Pum, Sc, Cpx, Afs, Obs ^{tr}, Gar ^{tr}	40	1.5	1.21	0.07	2.1	0.98
	Intonachino	Crypt., Anisotr.	Pum, Sc, CF	15	5.7	0.73	0.02	2.7	1.27
AB4	*Arriccio*	Crypt., Anisotr.	Pum, Sc, Afs, CF, Cpx ^{tr}, Amp ^{tr}	15	5.7	0.72	0.08	2.2	0.75
	Intonachino	Crypt., Isotr.	Cal, CF	20	4.0	0.35	0.02	3.6	1.07
AB5	*Arriccio*	Micr., Anisotr.	Pum, Sc, Cpx, Afs, Cer, Pl ^{tr}, Ol ^{tr}, CF^{tr}	40	1.5	1.19	0.04	2.2	0.94
	Intonachino	Crypt., Anisotr.	Cer, CF, Cpx ^{tr}, Afs ^{tr}	25	3.0	0.62	0.05	2.2	0.83
AB6	*Arriccio*	Crypt., Anisotr.	Pum, Sc, Cpx, Afs, Amp, Gar ^{tr}, CF ^{tr}	35	1.9	0.73	0.09	2.3	0.72
	Intonachino	Micr., Anisotr.	MF, Cal	45	1.2	1.44	0.04	2.8	1.31
AB7	*Arriccio*	Crypt., Anisotr.	Cpx, Obs, Pum, Sc	35	1.9	0.83	0.08	2.3	0.85
	Intonachino	Micr., Anisotr.	MF, Cal, Pum ^{tr}, Sc ^{tr}	45	1.2	1.05	0.05	2.3	0.96
AB8	*Arriccio*	Crypt., Anisotr.	Pum, Sc, Cpx, Afs, Obs, Cer, Gar ^{tr}	40	1.5	1.07	0.10	1.8	0.85
	Intonachino	Crypt., Anisotr.	Cer, CF, Pum, Sc, Obs ^{tr}, Cpx ^{tr}	25	3.0	1.01	0.05	2.2	0.92

Legend: Comparative charts were used for the determination of the percentage of aggregate via visual estimation; B/A, binder-to-aggregate ratio (determined by volume). Abbreviations: crypt, cryptocrystalline; micr, microcrystalline; isotr, isotropic; anisotr, anisotropic; pum, pumices; sc, scoriae; obs, obsidians; afs, alkali feldspar; qz, quartz; pl, plagioclase; cpx, clinopyroxene; amp, amphibole; ol, olivine; gar, garnet; cal, calcite; bt, biotite; cer, ceramic fragments; MF, marble fragments; CF, carbonate fragments; av, average; φ_{mF}, phi minimum Feret; S(φ_{mF}), standard deviation of phi; ^{tr}, traces.

4.1.1. *Cocciopesto*

Samples AB2, AB5 and AB8 are characterised by the presence of two overlapping layers (*arriccio* and *intonachino*) without a coloured pictorial decoration; actually, only a whitish (finishing) surface of few tens of micrometres was observed. On the light-orange- or pinkish-grey *arriccio* layer, with a thickness $\geq$ 0.8 cm, the *intonachino* was applied, which is thinner (0.4–0.7 cm) and lighter in colour (Table 1; Figure 3). The nature of the aggregate observed in all these mortars permitted to classify them as *cocciopesto*. Indeed, ceramic fragments were added in all samples; this aggregate showed some peculiarities in sample AB2, where it appeared coarser and more angular (Figure 3a–c; Table 2).

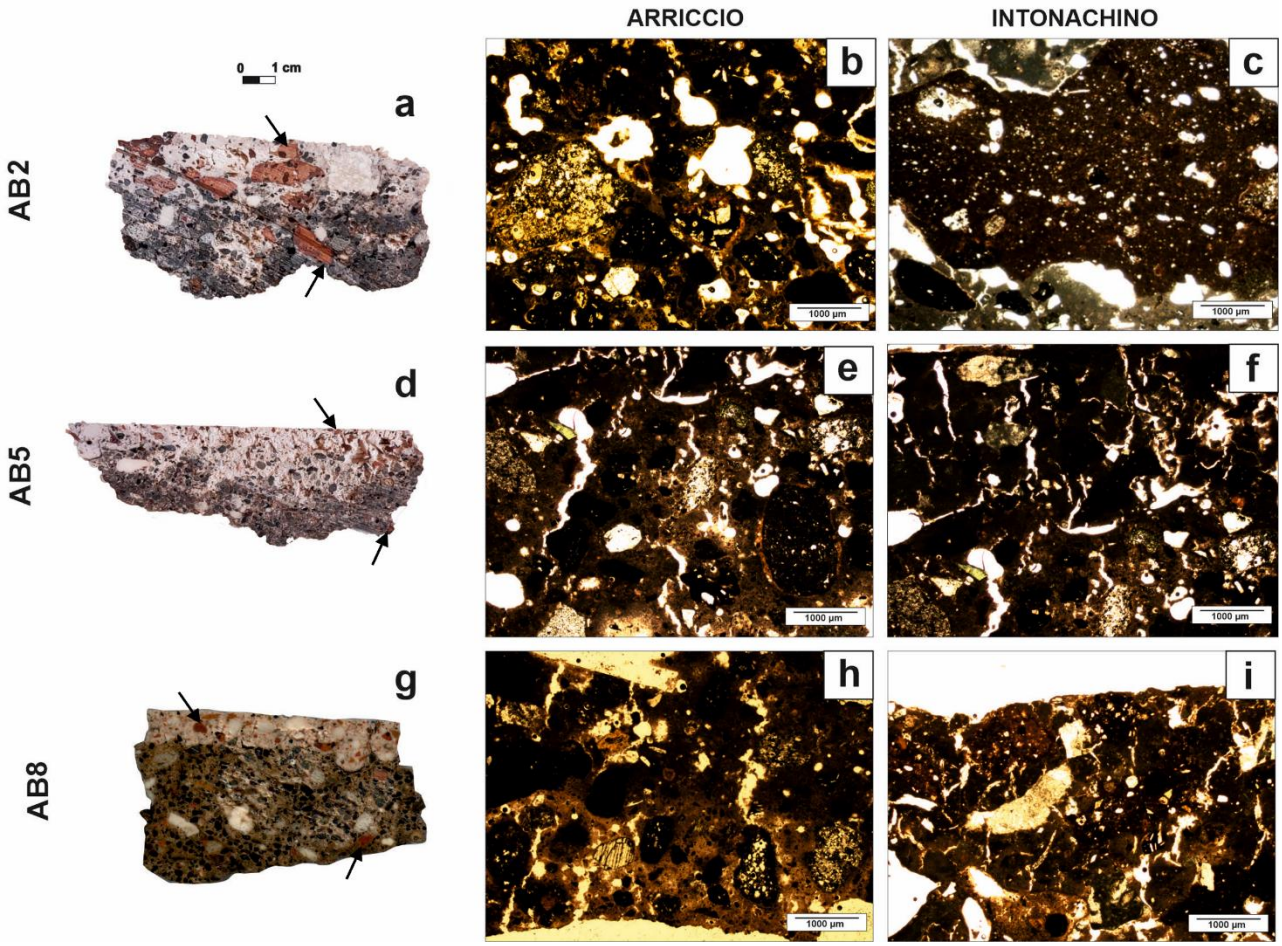

Figure 3. Stratigraphic sections of *cocciopesto* samples, showing the *arriccio* and in *intonachino* layers characterised by the presence of ceramic fragments (indicated by the arrows in the stratigraphic sections of samples) as aggregate, coarser in the sample AB2 sample (**a**–**c**), finer in the samples AB5 (**d**–**f**) and AB8 (**g**–**i**).

Here, in both *arriccio* and *intonachino* layers, coarse ceramic fragments (up to 1.9 cm) containing tiny quartz, alkali-feldspar, and rarer volcanic grains (ca. 30%) scattered in a red, anisotropic ceramic matrix were mixed with the binder. Along with ceramic fragments, a poorly sorted volcanic aggregate with sandy dimension (average φ_{mF} = 1.7–2.6, respectively) was recognised in the birefringent, microcrystalline binder (Table 2). It consists of pumice, scoriae, clinopyroxene, alkali feldspar, traces of olivine and quartz (Table 2).

Arriccio and *intonachino* layers of samples AB5 and AB8, collected from the inner plaster layers of room M, are, instead, characterised by the presence of finer (ranging from 0.07 to 0.40 cm) fragments of ceramics, differing from those observed in AB2 for their (unimodal) texture given by fine crystals of residual quartz and feldspar scattered in the anisotropic red matrix (Figure 3d–i).

The *arriccio* consists of a microcrystalline birefringent binder mixed to ceramic and volcanic aggregate (juveniles, clinopyroxene, alkali feldspar, traces of plagioclase, olivine, garnet) and rare carbonate fragments (ca. 40%), whereas in the *intonachino* the ceramic fragments were mixed to limestones and rare volcanic grains (ca. 25%) (Table 2).

Arriccio and *intonachino* layers showed frequent unmixed lumps in the binder, which reacted with aggregate, as proved by the presence of evident Si- and Al-bearing reaction rims edging both ceramic and volcanic glass fragments (Figure S1). The nature of the binder was investigated via SEM-EDS, which revealed the use of rather pure limestones, as testified by the chemical analyses performed on lime lumps, on which almost entirely CaO was detected (Table 3). However, values of Hydraulic Index [HI = (SiO_2 + Al_2O_3 + Fe_2O_3)/(CaO + MgO)] [19,20] calculated on

the binder range from 0.01 to 0.24, since variable contents of SiO_2, Al_2O_3, and Fe_2O_3 were detected on different portions of the binder, as a result of the interaction of lime with silico-aluminate aggregate.

Table 3. Compositional features of lime lumps and binders of representative samples. Hydraulic index (HI) was also calculated.

ID Sample	Layer	MgO	Al_2O_3	SiO_2	ClO	CaO	FeO_2	SO_3	HI
AB 3	*arriccio*	0.50	3.36	5.64	0.50	89.55	0.97	0.00	0.11
		0.33	2.07	3.29	0.47	93.30	0.45	0.56	0.06
		0.51	4.00	5.78	0.40	88.04	0.94	0.73	0.12
		1.49	2.80	5.52	0.00	90.18	0.00	0.00	0.09
		1.25	6.02	11.45	0.36	78.64	2.67	0.00	0.25
		1.04	3.40	6.24	0.43	88.43	0.89	0.00	0.12
							on average		0.13
	intonachino	0.69	4.50	2.39	0.60	92.40	0.00	0.00	0.07
		1.04	1.33	2.70	0.46	94.95	0.00	0.00	0.04
		0.65	1.13	2.34	0.45	95.45	0.42	0.00	0.04
		0.64	1.13	2.76	0.41	94.96	0.00	0.54	0.04
		0.55	1.06	2.02	0.41	95.91	0.00	0.46	0.03
		0.67	1.72	3.05	0.38	93.44	0.38	0.72	0.05
							on average		0.05
	lumps	0.00	0.52	0.65	0.35	98.83	0.00	0.00	0.01
		0.00	0.54	0.00	0.28	99.46	0.00	0.00	0.01
		0.00	0.62	0.40	0.34	98.98	0.00	0.00	0.01
							on average		0.01
AB 6	*arriccio*	0.69	2.53	4.50	0.37	91.55	0.71	0.00	0.08
		0.00	2.82	6.14	0.39	90.62	0.45	0.00	0.10
		0.51	3.87	4.56	0.49	91.06	0.00	0.00	0.09
		0.00	3.20	4.17	0.49	92.05	0.60	0.00	0.09
		0.00	3.10	4.29	0.51	92.06	0.55	0.00	0.09
		0.00	2.66	3.97	0.53	93.35	0.00	0.00	0.07
		0.00	1.13	3.19	0.00	95.70	0.00	0.00	0.05
							on average		0.08
	intonachino	0.40	2.31	4.83	0.46	91.87	0.58	0.00	0.08
		2.28	1.45	2.95	0.40	93.34	0.00	0.00	0.05
		0.79	2.42	2.52	0.48	94.26	0.00	0.00	0.05
		0.00	1.33	1.94	0.45	96.72	0.00	0.00	0.03
		0.00	1.45	2.19	0.46	95.82	0.53	0.00	0.04
		0.00	1.72	3.17	0.40	95.11	0.00	0.00	0.05
							on average		0.05
	lumps	0.42	0.67	0.42	0.23	98.50	0.00	0.00	0.01
		0.00	0.29	0.29	0.21	99.41	0.00	0.00	0.01
							on average		0.01

Table 3. *Cont.*

ID Sample	Layer	MgO	Al_2O_3	SiO_2	ClO	CaO	FeO_2	SO_3	HI
AB 8	*arriccio*	0.81	4.03	6.01	0.54	88.21	0.97	0.00	0.12
		0.00	5.09	6.86	0.58	86.40	1.33	0.32	0.15
		0.47	4.76	8.46	0.93	85.08	1.19	0.00	0.17
		0.00	0.45	0.45	0.28	99.07	0.00	0.00	0.01
		0.60	10.13	7.33	0.70	80.73	1.17	0.00	0.23
		0.00	11.17	7.41	0.52	80.52	0.90	0.00	0.24
							on average		0.15
	intonachino	1.09	2.29	3.33	0.35	93.29	0.00	0.00	0.06
		0.84	4.79	2.55	0.42	91.82	0.00	0.00	0.08
		0.97	3.03	4.59	0.48	90.64	0.76	0.00	0.09
		0.69	1.01	1.46	0.48	96.81	0.00	0.00	0.03
		0.51	0.76	0.96	0.45	97.50	0.00	0.28	0.02
		0.39	1.01	1.29	0.42	97.06	0.00	0.25	0.02
							on average		0.05
	lumps	0.00	0.24	0.48	0.00	99.15	0.13	0.00	0.01
		0.00	0.36	0.27	0.00	99.37	0.00	0.00	0.01
		0.00	0.45	0.45	0.28	99.07	0.00	0.00	0.01
							on average		0.01

4.1.2. Pozzolanic Plasters

Plasters from rooms I and L (i.e., samples AB1, AB3, and AB4) are characterised by three layers consisting of *arriccio*, an overlying layer of *intonachino*, and a pictorial layer on the surface (Figure 4a–i). The composition of aggregate observed via macroscopic observation and thin sections investigation allowed us to classify them as pozzolanic plasters.

The *arriccio* layer (from 1.7 to 0.7 cm thick; Table 1) of all samples, indeed, was prepared by adding to the birefringent microcrystalline binder a volcanic aggregate, consisting of volcanic glass fragments (pumices, scoriae, obsidians), crystals of clinopyroxene, alkali-feldspar, scarce plagioclase, and rare olivine, amphibole, garnet and quartz in variable percentages (B/A ranging from 5.7 to 1.5) (Figure 4; Table 2). It appears granulometrically heterogeneous, with dimension of grains variable between 0.02 and 1.21 mm (Table 2).

The *intonachino* layer (from 0.2 to 1.0 cm thick; Table 1), also acting as a preparatory layer for the application of the paint, is made of a lime-based binder containing carbonate rock fragments and calcite crystals, with scarcer pumices and scoriae (abundance variable from 10 to 30%) (Figure 4; Table 2). The dimension of the aggregate ranges from 0.99 to 0.02 mm (Table 2). Unmixed lumps were observed both in the *arriccio* and *intonachino* layers, more frequently in samples AB3 and AB4 (Table 1). As observed in the *cocciopesto*, lime lumps are composed mainly of CaO (98.50–99.46 wt.%, HI = 0.01), whereas the binders showed lower amounts of CaO + MgO (78.89–96.45 wt.%) and higher contents of SiO_2 + Al_2O_3 + Fe_2O_3 (3.08–20.13 wt.%) (Table 3). HI ranges from 0.03 to 0.25 (Table 3).

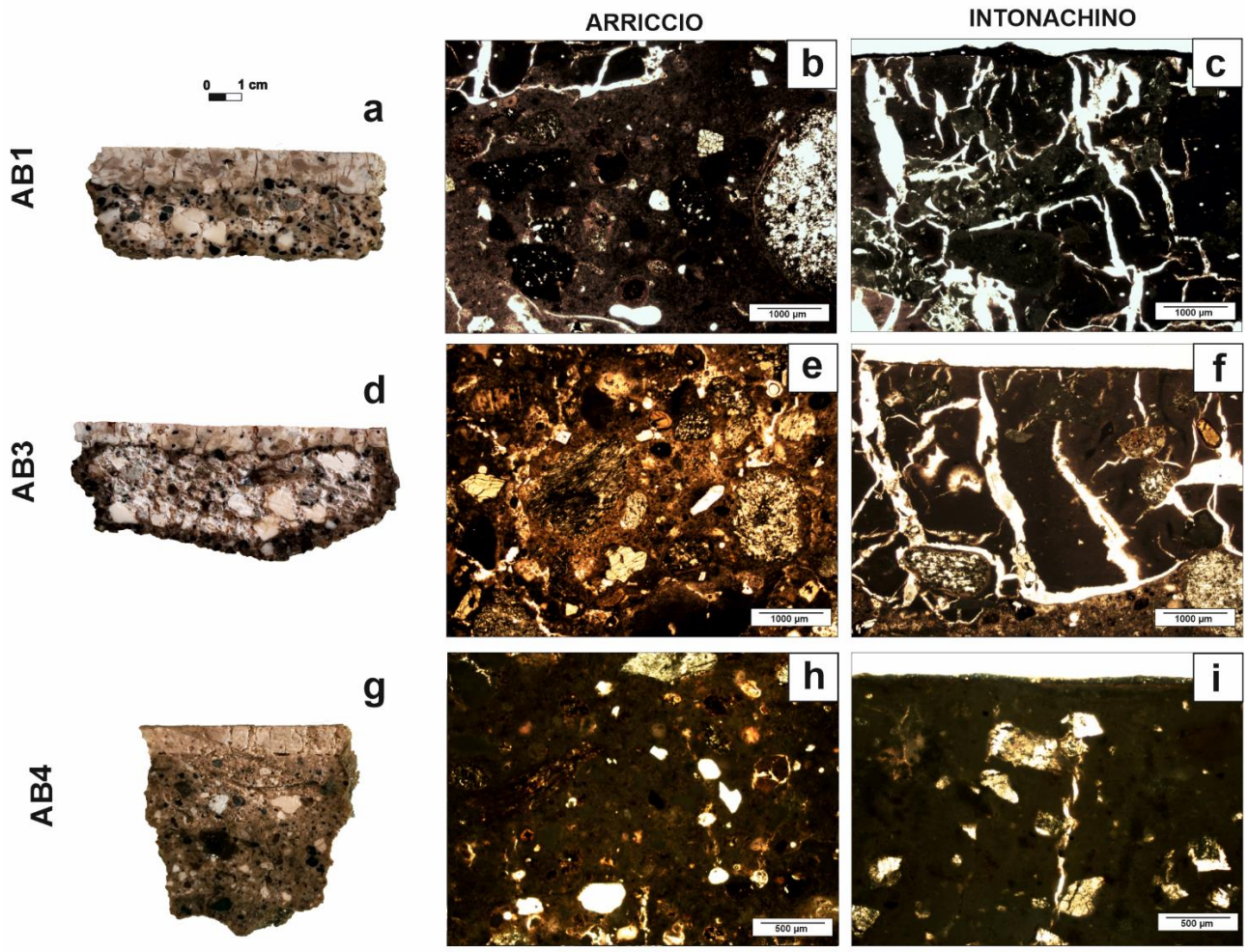

Figure 4. Stratigraphic sections of pozzolanic plasters containing volcanic aggregate, visible both in the *arriccio* and *intonachino* layers. (**a**–**c**) sample AB1; (**d**–**f**), sample AB3; (**g**–**i**) sample AB4.

4.1.3. *Marmorino*

On plasters sampled on the outer layer of room H1, the *arriccio*, the *intonachino*, and the pictorial surface were recognised (Table 1). However, the characteristic feature of the samples collected (AB6 and AB7) is the presence of marble dust that allowed us to classify them as *marmorino* (Figure 5a–f).

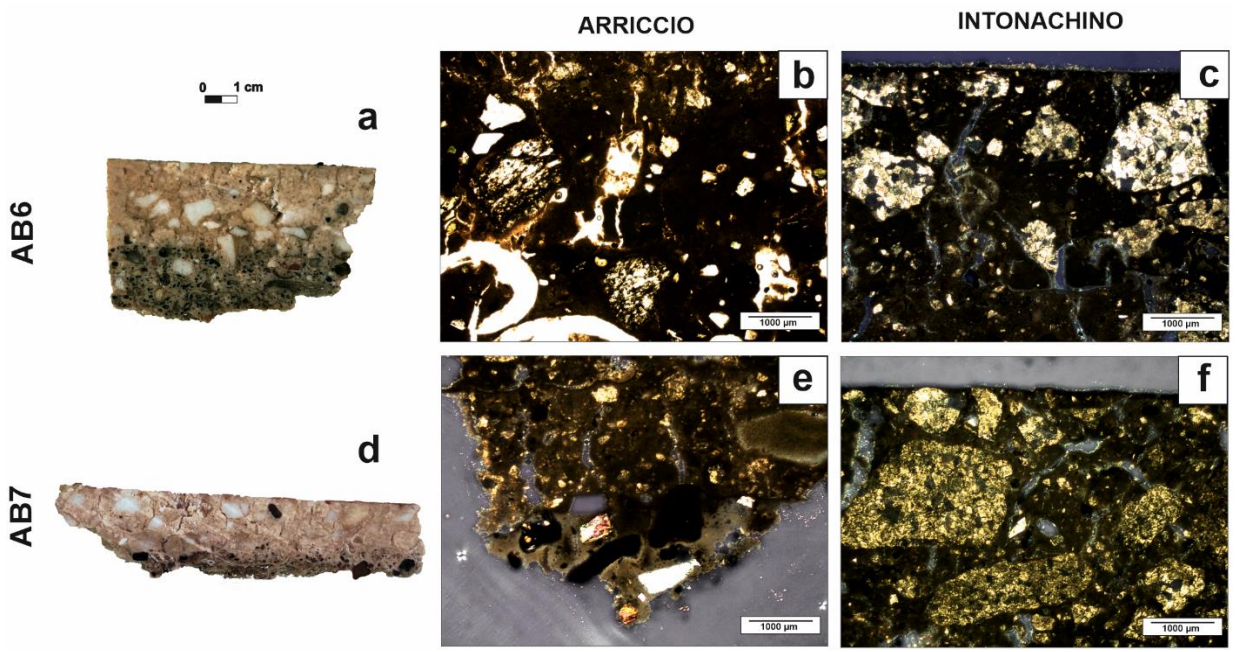

Figure 5. Stratigraphic sections of *marmorino* samples, made with lime binder in which volcanic aggregate was mixed into the *arriccio* and marble dust into the *intonachino*. (**a**–**c**) sample AB6; (**d**–**f**) sample AB7.

On the *arriccio* layer, composed of volcanic aggregate (juveniles, clinopyroxene, alkali-feldspar, traces of garnet and amphibole) mixed to the lime binder, the *intonachino* (0.6–1.0 cm) was made by adding to the binder a powder of marble fragments (ca. 40%) (Figure 5c,f), with dimensions variable from 1.44 to 0.04 mm (Table 2).

As observed for the other samples, the addition of aggregate improved the hydraulicity of the mixture (HI variable from 0.03 to 0.10; Table 3), which remains, evidently given the purely carbonate nature of the aggregate, always within very low values, indicating the aerial nature of the binder and the final mixture.

4.2. Pictorial Layers and Pigments

The thin pictorial layers coating the *intonachino* of pozzolanic mortars had a range of thickness between 60 and 120 µm. Except for the sample AB7, the decorated plasters showed two overlapping layers of different colours, revealing some care in the execution of the wall paintings.

In particular, AB1 shows red decoration on a white background (Figure 6a–d), AB3 presents red and orange bands on a yellow background (Figure 6e–h), as the result of a first application of the yellow pictorial layer and a later decoration with the other colours, whereas AB4 and AB6 are characterised by the application of a blue colour on a pink layer, directly spread on the underlying plaster (Figure 6i–p). AB7, instead, is characterised by the presence of a dark red surface (Figure 6q–t). The results, as reported below, converge to the identification of the main pigments used to decorate the surfaces.

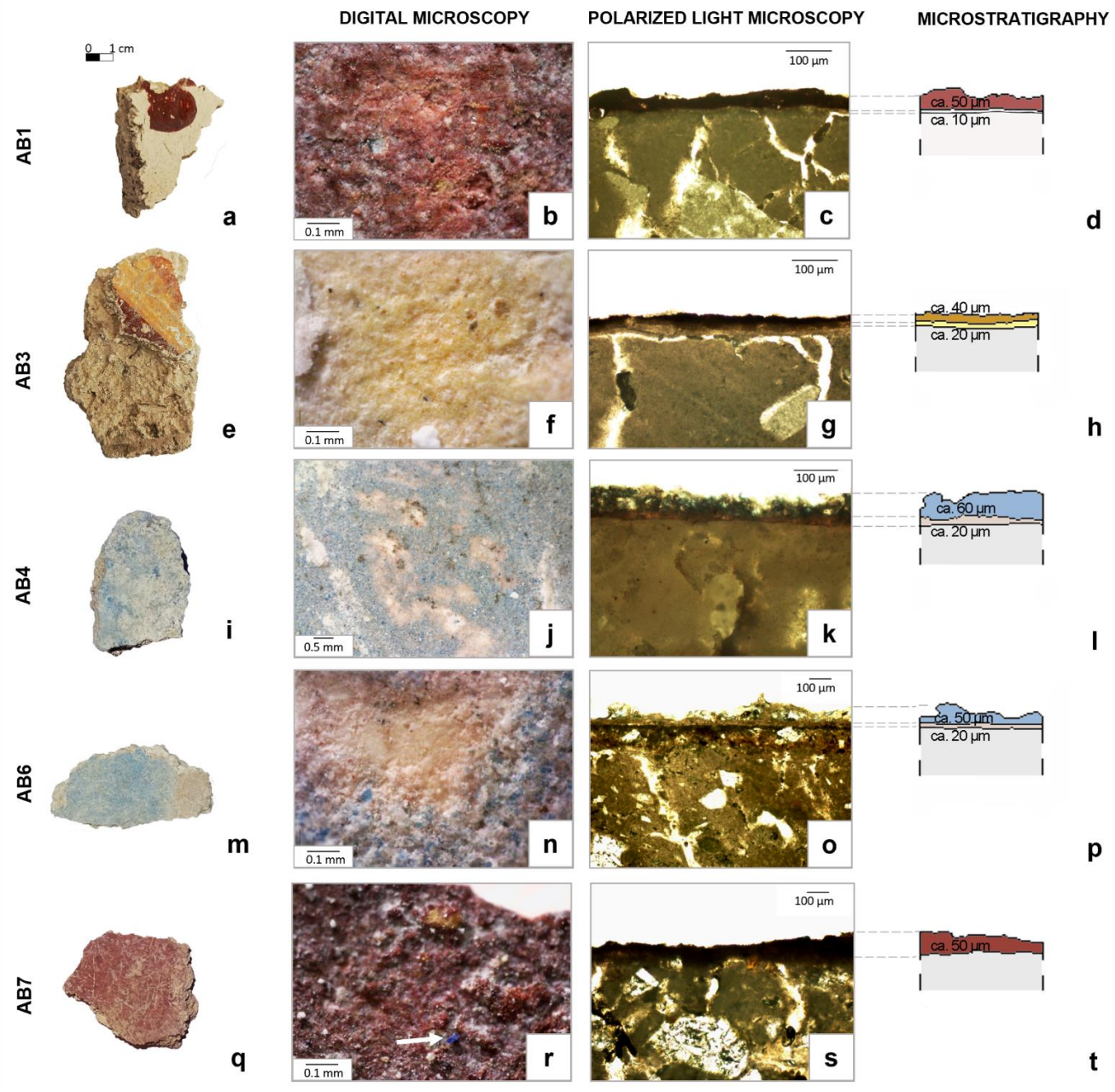

Figure 6. From macro to micro: pictorial layers of the samples AB1 (**a**–**d**), AB3 (**e**–**h**), AB4 (**i**–**l**), AB6 (**m**–**p**), AB7 (**q**–**t**) under Digital and Polarized Light Microscopy, with their microstratigraphic sketch.

4.2.1. White Surfaces

White colour was observed as the background of the red decorations on samples AB1 (Figure 6a), as well as on the surfaces of samples AB2, AB5, and AB8. XRF spectrum, acquired on the white portion of the sample AB1, indicates that calcium was the main element constituting such a colour (Figure 7; Table 4). ATR-FTIR spectroscopy revealed characteristic bands of calcium carbonate (Figure 7; Table 4). Infrared spectrum, in fact, is featured by the presence of a strong band at 1795 ($\nu_1 + \nu_4$ combination mode), 1410 (C-O asymmetric stretching vibration), 873 ("out-of-plane" bending vibration in CO_3^{2-}) and 713 cm^{-1} ("in-plane" bending vibration in CO_3^{2-}) [21].

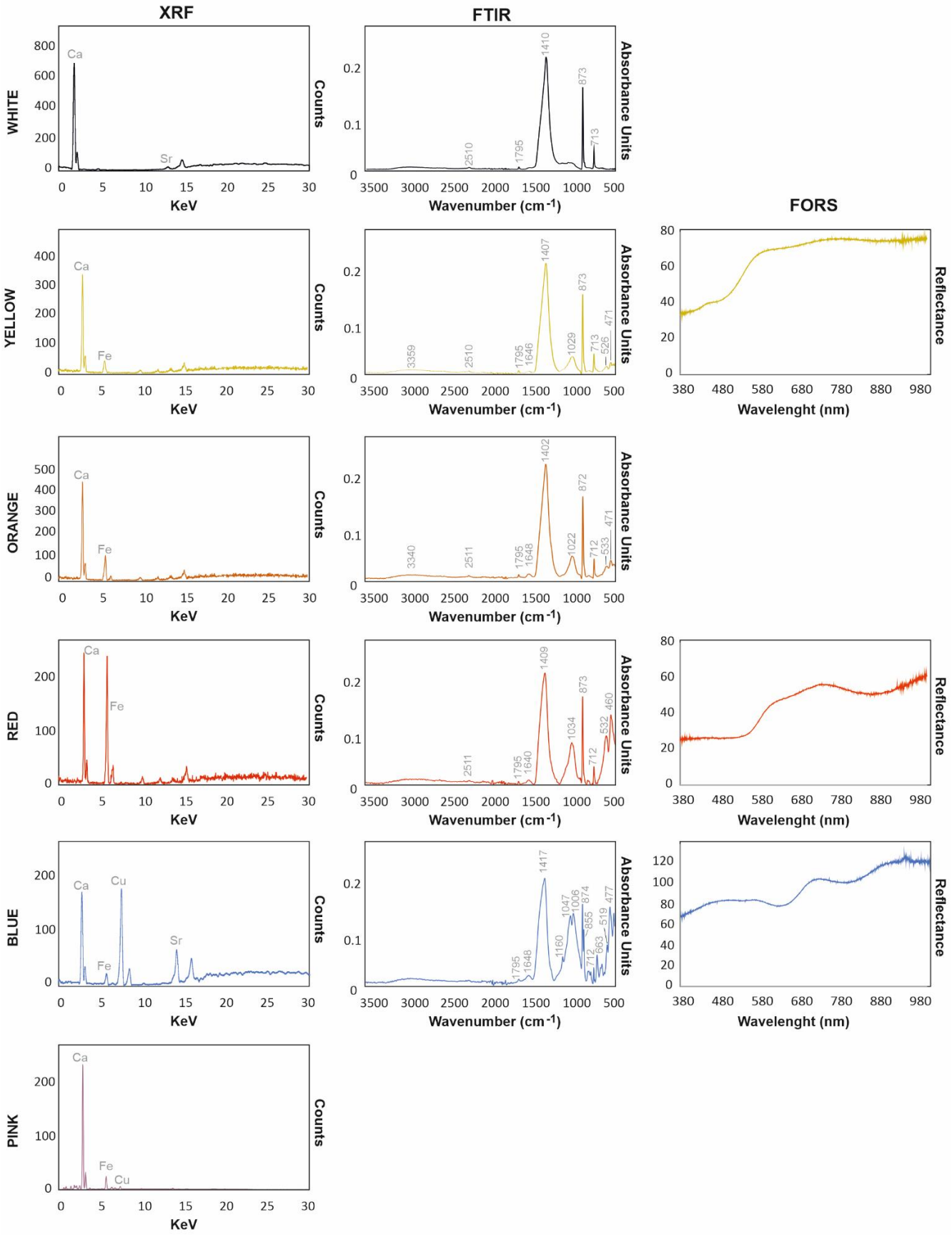

Figure 7. Representative spectra of the analysed colours obtained via pXRF, ATR-FTIR and FORS spectroscopy.

Table 4. Results of spectroscopic analyses performed on pictorial layers, with the indication of pigments identified and visual colour rendering (in RGB).

Sample	Colour	Colorimetric Coordinates			RGB Colour	XRF	FTIR (cm^{-1})	FORS (nm)	Pigment
		L*	a*	b*					
AB 1	White	-	-	-	-	Ca, Sr ^{tr}	2510, 1795, 1410, 873, 713	-	Calcite
	Red (on White)	66.07	16.29	11.37		Ca, Fe	1795, 1640, 1409, 1034, 873, 712, 692, 532, 460	~590, ~700	Red Ochre
AB 3	Yellow	87.71	8.36	24.36		Ca, Fe	3359, 2517, 1795, 1646, 1407, 1029, 872, 712, 526, 471	660, 930	Yellow ochre
	Red (on Yellow)	-	-	-	-	Ca, Fe	3351, 1795, 1640, 1409, 1167, 1034, 873, 797, 779, 712, 692, 532, 460	-	Red Ochre
	Orange (on Yellow)	-	-	-	-	Ca, Fe	3340, 2511, 1795, 1648 1402, 1022, 872, 712, 533, 471	-	Red Ochre + Yellow Ochre
AB 4	Blue (on Pink)	82.77	0.09	3.05		Cu, Ca, Fe, Sr	1795, 1648, 1417, 1160, 1047, 1006, 874, 855, 754, 712, 663, 593, 519, 477	630, 800	Egyptian blue
	Pink	-	-	-	-	Ca, Cu, Fe	-	-	Red ochre + calcite
AB 6	Blue (on Pink)	91.07	−2.08	4.89		Cu, Ca, Fe, Sr	1795, 1649, 1414, 1160, 1048, 1010, 874, 712, 664, 519, 477	630, 800	Egyptian blue
	Pink	-	-	-	-	Ca, Fe	-	-	Red ochre + calcite
AB 7	Red	79.24	6.65	5.84		Ca, Fe, Cu ^{tr}, Sr ^{tr}	1795, 1408, 1032, 873, 712, 546, 470	~590, ~700	Red Ochre

Legend: (^{tr}, traces).

4.2.2. Yellow Colour

The painted yellow decoration was examined in sample AB3 (Figure 6e). Digital microscope observation revealed the presence of white particles and very small dark red spots in a yellow matrix (Figure 6f). XRF elemental analysis detected the presence of predominant iron and calcium (Table 3). Along with the bands of calcium carbonate at 1795, 1407, 873 and 713 cm^{-1}, FTIR spectrum shows some absorbance peaks at 3359 (O-H stretching vibration) and 1646 cm^{-1} (O-H bending vibration) due to the presence of water in hydrated mineralogical phases (e.g., clayey minerals) [22], the infrared bands at 1029 cm^{-1} due to the Si-O-Si vibration in silicates [23], and the peaks at 526 and 471 cm^{-1}, which are likely linked to Fe-O vibration in the iron oxides [24], visible as small dark red spots by digital microscopy (Figure 6f). Such a mineralogical assemblage allowed us to infer the use of a naturally yellow earth pigment. FORS analysis confirms this hypothesis, showing a reflectance curve characterised by a typical S-shape that presents two broad absorption bands near 660 nm and 930 nm which could be attributed to goethite [25].

4.2.3. Orange Colour

The orange colour was used for the banded pictorial decoration preserved in the sample AB3 (Figure 6e). It was applied over the yellow background paint and, because of the small-sized area decorated with this colour, we were not able to perform FORS analysis. However, the pigment was observed via digital microscopy, which highlighted the mixture of red and yellow grains giving the orange pigmentation. Calcium and iron were detected by XRF (Table 4), whereas FTIR showed the bands of iron-based pigments (i.e., ochre) at 3340, 1648, 1022, 533, and 471 cm^{-1}, along with the bands of calcium carbonate (Figure 7).

4.2.4. Red Colour

The dark red colour was observed on AB1, AB3 and AB7 fragments (Figure 6a,e,q). In samples AB1 and AB3 the red pigment (Table 4), overpainted on the white and yellow backgrounds, respectively, appears homogeneous and intense in colour (AB1: L* = 66.07; a* = 16.29; b* = 11.37; Figure 6b). XRF spectroscopy on sample AB1 and AB3 shows the presence of calcium and iron (Figure 7; Table 4).

On the other hand, in the sample AB7 the dark red surface (L* = 79.24; a* = 6.65; b* = 5.84; Table 4) presents very small pink spots and blue particles (white arrow in Figure 6r), responsible of the presence of copper in XRF spectrum (Table 4).

The small blue particles visible on the surface, however, were not likely used as a mixture to create a particular shade of colour, as it usually did in the ancient world [17,26,27], but rather they could be traces of some kind of decoration no longer preserved (traces of brush strokes were visible on the surface of room M).

The reflectance curves of red pictorial surface of AB1 and AB7 samples are characterised by two main slopes at around 590 nm and 700 nm specific for haematite (Figure 7) [28,29]. In all samples, FTIR spectra showed the strong peaks of calcium carbonate at ca. 1795, 1408, 873 and 713 cm^{-1} and the infrared bands at ca. 1032, 540 and 465 cm^{-1}, along with the peaks at 3351 and 1640 cm^{-1} in the sample AB3, due to the presence of silicates and iron oxides (Figure 7; Table 4) typical of red ochre pigment [23,30]. Furthermore, the presence of lower quartz was proved by the bands at ca. 1167, 798, 780, and 695 cm^{-1} [31] (Figure 7; Table 4).

4.2.5. Blue Colour

Two samples (AB4 and AB6, Figure 6i,p) are characterised by a light blue pictorial layer. In both samples, the poor preservation of the blue layer permitted the observation of a pink, underlying paint layer below the blue (Figure 6j,n). Optical microscope observations highlighted the microstratification of the pictorial layers, with an underlying pink layer on which the paint composed of blue particles in a white medium was spread (Figure 6k,o).

Spectroscopic techniques permitted the clear identification of the blue pigment, which consists of Egyptian blue. XRF, in fact, detected copper along with calcium and lower amounts of iron and strontium; FORS curves showed a slope after a wavelenght of 580 nm, two absorption bands near 630 nm and 800 nm and the peak at 950 nm, which could be assigned to infrared fluorescence typical of Egyptian blue pigment [32,33]; FTIR spectra were featured by the typical bands at ca. 1160, 1047 and 1006 cm^{-1} [17] (Figure 7; Table 4). The FTIR analysis showed, in addition to the bands of the blue pigment, the peaks of calcite and the presence of aragonite in the sample AB4, as proved by the band at 855 cm^{-1} [34] (Figure 7; Table 4).

4.2.6. Pink Colour

The pink hue was observed as a background of the blue decoration of room M, preserved in the samples AB4 and AB6. Unfortunately, the features of the pink layer could only be observed in the areas where the blue layer was removed.

On the surfaces painted in pink, red spots are scattered in the white medium, to give them a peach-coloured aspect (Figure 6j,n). However, the small size of the interested surface only allowed us to perform XRF analyses, which revealed the presence of iron along with calcium (Figure 7; Table 4), suggesting a mixing of Fe-based pigment in a medium made of calcite. Moreover, XRF detected copper, likely due to residual traces of blue pigments on the investigated surfaces.

5. Discussion

The study of decorated plasters of the early imperial *domus* of *M. Vipsanius Primigenius* in *Abellinum* by means of a combined use of spectroscopic and microscopic techniques provided useful information to solve the issues concerning plastering technology and use of pigments adopted for decorating the *domus*.

5.1. Technology of Plastering

Archaeometric analyses revealed interesting information on the technology of plastering used in the *domus* of *Abellinum*. In fact, although the type of the binder is rather similar, the type of aggregate observed in the wall fragments (volcanic grains for pozzolanic plasters, ceramic fragments for *cocciopesto*, and marble dust for *marmorino*) revealed different technological choices consistent with those already observed in the *Campania* region in the same historical context [1,35,36].

The plasters of rooms H and L are pozzolanic plasters. They were obtained by adding volcanic aggregate (juveniles, crystals of clinopyroxene, alkali-feldspar, traces of olivine, garnet, and amphibole) into the lime binder to make the innermost layer, namely the *arriccio*, which directly adhered on the tuff masonries. On it, a lime-based layer containing limestones fragments and calcite crystals as aggregate was spread (i.e., *intonachino*) to hold the pigments; in fact, any real preparation layer is lacking.

The addition of natural *pozzolana* responds to the need to increase the hydraulicity of the plaster and, consequently, the resistance of the final mixture. The presence of this type of material, indeed, increases the hydraulicity considerably, as the re-active silica contained in the pozzolanic material reacts with the calcium hydroxide, leading to the formation of insoluble products with binding properties, namely calcium silicate hydrates (C-S-H phases) [37]. These phases, in the aged binders exposed to long-term variable humidity, may carbonate, originating metastable $CaCO_3$ aragonite (and also vaterite) polymorph [38,39]. It might explain the presence of aragonite in the sample AB4 (Table 4).

The hydraulicity is, therefore, correlated to the presence of pozzolanic aggregate in the binder, obtained by a rather pure limestone, as proved by the microchemical analyses of unmixed lumps, which preserved the compositional features of the original rock used to produce the latter. The higher values of HI calculated on different areas of the binder (Table 3) are the result of the pozzolanic reaction occurred between the silica-rich volcanic grains and the lime, as testified by the evident reaction rims edging the aggregate particles. The detection of low SO_3 (Table 3), instead, suggest possible sulphation phenomena affecting the samples.

Regarding the origin of raw materials, data so far acquired did not permit us to exactly locate the sources of limestones used to produce the binder (suitable limestones largely outcrops in *Campania* region [40]); volcanic aggregate, instead, was likely collected nearby to the site, where volcanic-rich detritic-colluvial and fall deposits define the top of the tuff dome where *Abellinum* was built [10]. The geological nature of such a natural deposit justifies the mixing of volcanic and siliciclastic grains observed as aggregate in the pozzolanic mortars (Table 2).

The plasters of rooms I and M, instead, are characterised by different mineralogical and textural features. Although the same wall typology (*opus reticulatum*) and the contemporaneity of the two rooms, in room I the technology of plastering radically changes, likely in response to demanding renovations that required the re-plastering of the room. The walls are covered with a plaster containing large ceramic fragments to make the *cocciopesto*.

The use of crushed ceramic material as reactive additives in Roman period mortars is well known as a means of producing hardwearing wall covering [41]. A variety of broken ceramic objects, from ceramic building materials (tile and bricks) to amphorae and common wares (cooking and table ware) were usually added to the slaked lime to produce a stronger and more waterproof set [41]. In this case, the rather fine texture of ceramic fragments meant that the crushing and grinding of ceramic building materials was not performed; rather, there could also be the crushing and pulverization of common wares into a fine powder. Minero-petrographic features did not provide enough information for determining their provenance, but they represent a testimony of the re-use of ceramic waste materials in preparations of mortars.

The same type of aggregate was observed in room M; in particular, this area is featured by two overlapping plaster layers, the innermost made with *cocciopesto* (where the ceramic fragments are visibly smaller) (Figure 3d–i), and the outermost layer made with *marmorino*.

The outer layer of the room, in fact, was plastered with lime binder containing volcanic aggregate in the *arriccio* and marble powder in the *intonachino* (Figure 5).

The presence of *marmorino* represents an effective indicator of the wealth of the *domus* also in the subsequent restructuring phase. In fact, the use of marble dust offers important technological implications: the function of marble grains, and of the aggregate in general, is to reduce the shrinkage that occurs during hardening and, mostly, to improve the mechanical properties of the resulting material [42]. In particular, due to its quite high fineness, marble powder proved to be very effective in assuring very good cohesiveness of the mortar [43]. Along with the technological advantages of marble powders, Vitruvius recommended the use of transparent grains of marble for at least three coats, if the intent was to give a white shine and lustre appearance to the plasters coating the walls [44,45].

5.2. Wall Painting Technique and Pigments

5.2.1. Painting Technique

As described before, the rooms of the *domus* were decorated in 3rd and 4th Pompeian style [12], with which the walls were likely entirely decorated. Archaeological excavations, however, unearthed the only basal part (about one meter from the floor) of the *domus*, characterised by decorations diversified in the various rooms.

Some of the collected samples have a pictorial stratification consisting of two layers, a background (white, yellow, or pink) and the superficial pictorial layer (red, orange, or blue). Evidently, the painting technique used to spread the colour on the wall surfaces differs according to the layer that the painter applied. In fact, the pictorial layer seems to be applied *a fresco* on the *intonachino*. The pigment was diluted in water and applied directly over damp plaster. In the process of drying and setting, the pigment was incorporated becoming an integral part of the underlying layer. In accordance, the chemical analyses always show the presence of calcium carbonate, and spectroscopic techniques detected the presence of calcite. Moreover, the microstratigraphic study revealed low thicknesses (less than 50 μm) for the first paint layers, which is consistent with *a fresco* application.

The overlying pictorial layers were applied at a later time, to complete the decoration or to add details. Spectroscopic techniques did not detect traces of organic binders mixed to the pigments used in these layers, but rather in all spectra calcium and evidence of calcite suggested the application using lime-painting technique. Thus, the pigments were mixed with slaked lime or limewater (lime-painting technique) that reactivate the carbonation process [7,46] incorporating in this way the pigment in a new painting layer rather than in the underlying preparatory layer.

5.2.2. Pigments: Natural and Synthetic Compounds

Both natural and synthetic pigments formed part of the palette of the painters of *Abellinum*. Natural pigments consisted of naturally occurring earth pigments. The spectroscopic analyses carried out on red, orange, yellow, and pink colours, in fact, highlighted the use of ochres, likely mixed together to obtain different shades, or diluted with the white pigment (calcite) to lighten the colour tones. The large availability of these pigments in geological environments has made them usable since the earliest expressions of human art [47].

The colouring matter of the raw material consists of iron oxides and/or hydroxides. Associated with these phases, quartz, clayey minerals, and carbonates can be also present in the deposit, also depending on the processing of the pigment. For the red, yellow, orange, and pink colours, the spectroscopic analyses detected the presence of iron, associated with Fe oxides, the main colouring matter of ochres, mainly along with (hydrated) silicates, in accordance with the natural origin of ochres [23,48]. The presence of the calcite is to be referred to the pictorial technique, as discussed above. FTIR results are consistent with the data collected by FORS, confirming the use of an earth-based pigment [49].

The only synthetic pigment used by the painters of the *domus* is Egyptian blue, the oldest known synthetic pigment dating back to the 3rd millennium BC, and the most

common among the blue colouring compounds used in the Mediterranean area during the Roman period [50–53]. Vitruvius, at the beginning of the 1st century BCE, in his Ten Books on Architecture [44], described the manufacture of Egyptian blue, informing of workshops also located in southern Italy [50,54]. The pigment continued to be used until the fall of the Roman Empire, when technological knowledge changed and Egyptian blue was replaced with lapis lazuli [55]. Nevertheless, recent studies have found an unexpected use of Egyptian blue in Renaissance works (e.g., Raphael *fresco* of Triumph of Galatea at *Villa Farnesina*, Rome [56]). Egyptian blue is also listed among the most expensive by Pliny, which confirms the refinement and wealth of the commissioner of the paintings [12].

The pigment was used to create a pictorial layer on a pink underlying background, as observed in the samples AB4 and AB6. Calcium and copper by chemical analyses, infrared bands of FTIR spectra, and reflectance curves related to electronic transitions attributable to Cu^{2+} ions obtained by FORS suggest the presence of cuprorivaite, the calcium-copper tetrasilicate ($CaCuSi_4O_{10}$) deriving from the synthesis of the pigment [57–59].

6. Conclusions

The archaeometric study of fragments of decorated plasters *domus* of *Marcus Vipsanius Primigenius* in *Abellinum* represented an important tool for broadening knowledge on the importance of the archaeological site, as well as on the ambitions of the *domus* owner and his social value. Although they were poorly preserved due to the collapse of the upper part, the walls remained in their original context. This permitted interesting information to be obtained about how the plasters were made and how they were decorated.

The walls made by *opus reticulatum* were plastered by using a multilayer technology, using different mix designs according to the type of aggregate mixed to the lime binder (*cocciopesto*, pozzolanic plasters and *marmorino*). The changing in the plastering technology was likely to respond to demanding renovations that required the re-plastering of the surfaces. On them, the pigments were applied *a fresco* to create a white, yellow, or pink background in-built with the underlying plasters; then, details to complete the decoration were applied by the lime painting technique. The palette consisted of natural (calcite, red, and yellow ochres) and synthetic pigments (Egyptian blue), occasionally mixed together to obtain different shades or lighten the colour tones.

Supplementary Materials: The following supporting information can be downloaded at: https://www.mdpi.com/article/10.3390/min12121487/s1, Figure S1: (a) Reaction rim around a pumice in the sample AB6; (b) detail of the reaction rim and EDS spectra of lime binder (spectrum 1), rim around the pumice (spectrum 2) and pumice (spectrum 3).

Author Contributions: Conceptualization, C.G. (Chiara Germinario) and C.G. (Celestino Grifa); Formal analysis, C.G. (Chiara Germinario) and M.F.A.; Funding acquisition, A.S. and C.G. (Celestino Grifa); Investigation, S.P., C.G. (Chiara Germinario), M.F.A. and S.S.; Methodology, C.G. (Chiara Germinario) and C.G. (Celestino Grifa); Project administration, A.S.; Resources, M.M., S.S. and C.G. (Celestino Grifa); Supervision, C.G. (Celestino Grifa); Visualization, S.P. and C.G. (Chiara Germinario); Writing—original draft, S.P., C.G. (Chiara Germinario) and C.G. (Celestino Grifa); Writing—review and editing, S.P., C.G. (Chiara Germinario), M.F.A., M.C., M.M., D.M., R.P., A.S., S.S. and C.G. (Celestino Grifa). All authors have read and agreed to the published version of the manuscript.

Funding: The research was supported by grants from the Department of Sciences and Technologies of University of Sannio to Celestino Grifa (FRA 2020 Celestino Grifa) and the Department of Cultural Heritage of University of Salerno to Alfonso Santoriello (300398CELSANTO_01-Carta Archeologica del centro storico Atripalda).

Data Availability Statement: The data presented in this study are available on request from the corresponding author.

Acknowledgments: The project is carried out in observance of the concessions MiBAC | DG-ABAP_SERV II_UO1 | 08/07/2019 | 0018628-P | [34.31.07/3.32.1/2018] and MIC_DG-ABAP_SERV II 01/06/2022 0020738-P [34.61.07/1.27.1/2019] (decreto DG-ABAP | 31/05/2022 | DECRETO 696)]. The authors kindly thank the *Soprintendenza Archeologia, Belle Arti e Paesaggio* of *Salerno* e *Avellino* provinces, for the collaboration in the scientific activities and the municipality of *Atripalda* for the logistic support.

Conflicts of Interest: The authors declare no conflict of interest.

References

1. Miriello, D.; Bloise, A.; Crisci, G.M.; De Luca, R.; De Nigris, B.; Martellone, A.; Osanna, M.; Pace, R.; Pecci, A.; Ruggieri, N. New compositional data on ancient mortars and plasters from Pompeii (Campania–Southern Italy): Archaeometric results and considerations about their time evolution. *Mater. Charact.* **2018**, *146*, 189–203. [CrossRef]
2. Piovesan, R.; Siddall, R.; Mazzoli, C.; Nodari, L. The Temple of Venus (Pompeii): A study of the pigments and painting techniques. *J. Archaeol. Sci.* **2011**, *38*, 2633–2643. [CrossRef]
3. Amadori, M.; Barcelli, S.; Poldi, G.; Ferrucci, F.; Andreotti, A.; Baraldi, P.; Colombini, M. Invasive and non-invasive analyses for knowledge and conservation of Roman wall paintings of the Villa of the Papyri in Herculaneum. *Microchem. J.* **2015**, *118*, 183–192. [CrossRef]
4. Di Benedetto, C.; Graziano, S.F.; Guarino, V.; Rispoli, C.; Munzi, P.; Morra, V.; Cappelletti, P. Romans' established skills: Mortars from D46b mausoleum, porta mediana necropolis, Cuma (Naples). *Mediterr Archaeol Archaeom.* **2018**, *18*, 131–146.
5. Graziano, S.F.; Rispoli, C.; Guarino, V.; Balassone, G.; Di Maio, G.; Pappalardo, L.; Cappelletti, P.; Damato, G.; De Bonis, A.; Di Benedetto, C.; et al. The roman villa of Positano (Campania region, Southern Italy): Plasters, tiles and geoarchaeological reconstruction. *Int. J. Conserv. Sci.* **2020**, *11*, 319–344.
6. Cuní, J. What do we know of Roman wall painting technique? Potential confounding factors in ancient paint media analysis. *Heritage Sci.* **2016**, *4*, 1–13. [CrossRef]
7. Salvadori, M.; Sbrolli, C. Wall paintings through the ages: The roman period—Republic and early Empire. *Archaeol. Anthr. Sci.* **2021**, *13*, 1–30. [CrossRef]
8. De Bonis, A.; Grifa, C.; Cultrone, G.; De Vita, P.; Langella, A.; Morra, V. Raw materials for archaeological pottery from the Campania region of Italy: A petrophysical characterization. *Geoarchaeology* **2013**, *28*, 478–503. [CrossRef]
9. Colucci Pescatori, G. Evidenze archeologiche in Irpinia. In *La Rom du Samnium aux IIe Ier s av J-C*; Bérard, C.J., Ed.; Centre Jean Bérard: Naples, Italy, 1991; pp. 85–122.
10. Pescatore, T.; Pinto, F. *Note Illustrative Della Carta Geologica d'Italia alla Scala 1:50.000*; Foglio 449-Avellino. Regione Campania; ISPRA, Servizio Geologico d'Italia: Roma, Italy, 2009.
11. Colucci Pescatori, G. Abellinum (Atripalda). Introduzione. In *Fana, Templa, Delubra Corpus dei Luoghi di Culto dell'Italia Antica-2 Reg I Avella, Atripalda, Salerno*; Cinquantaquattro, T., Colucci Pescatori, G., Eds.; Collège de France: Paris, France, 2013; pp. 27–34.
12. Rackham, H. *Pliny the Elder. Natural History in Ten Volumes*; Loeb Classical Library: Cambridge, MA, USA, 1968.
13. Fariello Sarno, M.R. Abellinum romana II. In *Stor Illus di Avellino e dell'Irpinia L'Irpinia Antica*; Colucci Pescatori, G., Ed.; Sellino & Barra: Salerno, Italy, 1996; pp. 113–119.
14. Johannowsky WGangemi, G.; Romito, M.; Colucci Pescatori, G.; Peduto, P.; Fariello Sarno, M.R. *Note Di Archeologia E Topografia Dell'irpinia Antica*; Edizioni del Centro Dorso: Avellino, Italy, 1987.
15. CNR-ICR. *UNI-EN 11176:2006, Cultural Heritage. Petrographic Description of a Mortar*; CNR-ICR: Rome, Italy, 2006.
16. UNI. *UNI 11305:2009, Beni Culturali-Malte Storiche-Linee Guida per la Caratterizzazione Mineralogico-Petrografica, Fisica e Chimica Delle Malte*; UNI: Milano, Italy, 2009.
17. Germinario, C.; Pagano, S.; Mercurio, M.; Izzo, F.; De Bonis, A.; Morra, V.; Munzi, P.; Leone, M.; Conca, E.; Grifa, C. Roman technological expertise in the construction of perpetual buildings: New insights into the wall paintings of a banquet scene from a tomb in Cumae (southern Italy). *Archaeol. Anthr. Sci.* **2022**, *14*, 1–17. [CrossRef]
18. Germinario, C.; Cultrone, G.; Cavassa, L.; De Bonis, A.; Izzo, F.; Langella, A.; Mercurio, M.; Morra, V.; Munzi, P.; Grifa, C. Local production and imitations of Late Roman pottery from a well in the Roman necropolis of Cuma in Naples, Italy. *Geoarchaeology* **2019**, *34*, 62–79. [CrossRef]
19. Boynton, R.S. *Chemistry and Technology of Lime and Limestone*; John Wiley & Sons: New York, NY, USA, 1966.
20. Charola, A.E.; Henriques, F.M.A. Hydraulicity in lime mortars revisited. In *Int RILEM Work Hist Mortars Charact Tests*; Paisley: Scotland, UK, 1999; pp. 95–104.
21. Germinario, C.; Izzo, F.; Mercurio, M.; Langella, A.; Sali, D.; Kakoulli, I.; De Bonis, A.; Grifa, C. Multi-analytical and non-invasive characterization of the polychromy of important archaeological wall paintings at the Domus of Octavius Quartio in Pompeii. *Eur. Phys. J. Plus.* **2018**, *133*, 359. [CrossRef]
22. Jozanikohan, G.; Abarghooei, M.N. The Fourier transform infrared spectroscopy (FTIR) analysis for the clay mineralogy studies in a clastic reservoir. *J. Pet. Explor. Prod. Technol.* **2022**, *12*, 2093–2106. [CrossRef]
23. Bikiaris, D.; Daniilia, S.; Sotiropoulou, S.; Katsimbiri, O.; Pavlidou, E.; Moutsatsou, A.; Chryssoulakis, Y. Ochre-differentiation through micro-Raman and micro-FTIR spectroscopies: Application on wall paintings at Meteora and Mount Athos, Greece. *Spectrochim. Acta A Mol. Biomol. Spectrosc.* **2000**, *56*, 3–18. [CrossRef] [PubMed]

24. Grifa, C.; Germinario, C.; De Bonis, A.; Langella, A.; Mercurio, M.; Izzo, F.; Smiljanic, D.; Guarino, V.; Di Mauro, S.; Soricelli, G. Comparing ceramic technologies: The production of Terra Sigillata in Puteoli and in the Bay of Naples. *J. Archaeol. Sci. Rep.* **2019**, *23*, 291–303. [CrossRef]
25. Cheilakou, E.; Troullinos, M.; Koui, M. Identification of pigments on Byzantine wall paintings from Crete (14th century AD) using non-invasive Fiber Optics Diffuse Reflectance Spectroscopy (FORS). *J. Archaeol. Sci.* **2014**, *41*, 541–555. [CrossRef]
26. Siddall, R. Not a day without a line drawn: Pigments and painting techniques of Roman Artists. *Infocus Mag.* **2006**, *2*, 18–31. [CrossRef]
27. Jorge-Villar, S.E.; Edwards, H.G.M. Green and blue pigments in Roman wall paintings: A challenge for Raman spectroscopy. *J. Raman Spectrosc.* **2021**, *52*, 2190–2203. [CrossRef]
28. Aceto, M.; Agostino, A.; Fenoglio, G.; Idone, A.; Gulmini, M.; Picollo, M.; Ricciardi, P.; Delaney, J.K. Characterisation of colourants on illuminated manuscripts by portable fibre optic UV-visible-NIR reflectance spectrophotometry. *Anal. Methods* **2014**, *6*, 1488–1500. [CrossRef]
29. Elias, M.; Chartier, C.; Prévôt, G.; Garay, H.; Vignaud, C.; Elias, M. The colour of ochres explained by their composition HAL Id: Hal-00848289 The colour of ochres explained by their composition. *Mater. Sci. Eng. B* **2021**, *127*, 70–80. [CrossRef]
30. Grifa, C.; Germinario, C.; De Bonis, A.; Cavassa, L.; Izzo, F.; Mercurio, M.; Langella, A.; Kakoulli, I.; Fischer, C.; Barra, D.; et al. A pottery workshop in Pompeii unveils new insights on the Roman ceramics crafting tradition and raw materials trade. *J. Archaeol. Sci.* **2021**, *126*, 105305. [CrossRef]
31. Mortimore, J.L.; Marshall, L.-J.R.; Almond, M.J.; Hollins, P.; Matthews, W. Analysis of red and yellow ochre samples from Clearwell Caves and Catalhoyok by vibrational spectroscopy and other techniques. *Spectrochim. Acta Part A Mol Biomol. Spectrosc.* **2004**, *60*, 1179–1188. [CrossRef] [PubMed]
32. Alberghina, M.F.; Germinario, C.; Bartolozzi, G.; Bracci, S.; Grifa, C.; Izzo, F.; La Russa, M.; Magrini, D.; Massa, E.; Mercurio, M.; et al. Non-invasive characterization of the pigment's palette used on the painted tomb slabs at Paestum archaeological site. *IOP Conf. Ser. Mater. Sci. Eng.* **2020**, *949*, 012002. [CrossRef]
33. Marey Mahmoud, H.H. Colorimetric and spectral reflectance access to some ancient Egyptian pigments. *J. Int. Colour. Assoc.* **2019**, *24*, 35–45.
34. Izzo, F.; Germinario, C.; Grifa, C.; Langella, A.; Mercurio, M. External reflectance FTIR dataset (4000–400 cm^{-1}) for the identification of relevant mineralogical phases forming Cultural Heritage materials. *Infrared Phys. Technol.* **2020**, *106*, 103266. [CrossRef]
35. Piovesan, R.; Curti, E.; Grifa, C.; Maritan, L.; Mazzoli, C. Petrographic & microstratigraphic analysis of mortar-based building materials from the temple of Venus, Pompeii. *Interpret. Silent. Artefacts Petrogr. Approaches Archaeol. Ceram. Archaeopress* **2009**, 65–80. [CrossRef]
36. Izzo, F.; Arizzi, A.; Cappelletti, P.; Cultrone, G.; De Bonis, A.; Germinario, C.; Graziano, S.F.; Grifa, C.; Guarino, V.; Mercurio, M.; et al. The art of building in the Roman period (89 B.C.–79 A.D.): Mortars, plasters and mosaic floors from ancient Stabiae (Naples, Italy). *Constr. Build. Mater.* **2016**, *117*, 129–143. [CrossRef]
37. De Luca, R.; Miriello, D.; Pecci, A.; Domínguez-Bella, S.; Bernal-Casasola, D.; Cottica, D.; Bloise, A.; Crisci, G.M. Archaeometric Study of Mortars from the Garum Shop at Pompeii, Campania, Italy. *Geoarchaeology* **2015**, *30*, 330–351. [CrossRef]
38. Black, L.; Breen, C.; Yarwood, J.; Garbev, K.; Stemmermann, P.; Gasharova, B. Structural features of C-S-H(I) and its carbonation in air-A Raman spectroscopic study. Part II: Carbonated phases. *J. Am. Ceram. Soc.* **2007**, *90*, 908–917. [CrossRef]
39. Frankeová, D.; Koudelková, V. Influence of ageing conditions on the mineralogical micro-character of natural hydraulic lime mortars. *Constr. Build. Mater.* **2020**, *264*, 120205. [CrossRef]
40. Vitale, S.; Ciarcia, S. Tectono-stratigraphic setting of the Campania region (southern Italy). *J. Maps* **2018**, *14*, 9–21. [CrossRef]
41. Siddall, R. From kitchen to bathhouse: The use of waste ceramics as pozzolanic additives in Roman mortars. In *Build Roma Aeterna Curr Res Rom Mortar Concr*; Ringbom, A., Hohlfelder, R.L., Eds.; The Finnish Society of Sciences and Letters: Helskinki, Finland, 2011; pp. 152–168.
42. Duran, A.; Perez-Maqueda, L.A.; Poyato, J.; Perez-Rodriguez, J.L. A thermal study approach to roman age wall painting mortars. *J. Therm. Anal.* **2010**, *99*, 803–809. [CrossRef]
43. Corinaldesi, V.; Moriconi, G.; Naik, T.R. Characterization of marble powder for its use in mortar and concrete. *Constr. Build. Mater.* **2010**, *24*, 113–117. [CrossRef]
44. Morgan, N.H. *Vitruvius. The Ten Books on Architecture*; Dover Publications: New York, NY, USA, 1960; p. 331.
45. Gutman, M.; Zupanek, B.; Kikelj, M.L.; Kramar, S. Wall Paintings from the Roman *Emona* (Ljubljana, Slovenia): Characterization of Mortar Layers and Pigments. *Archaeometry* **2015**, *58*, 297–314. [CrossRef]
46. Piovesan, R.; Mazzoli, C.; Maritan, L.; Cornale, P. Fresco and lime-paint: An experimental study and objective criteria for distinguishing between these painting techniques. *Archaeometry* **2012**, *54*, 723–736. [CrossRef]
47. Schmandt-Besserat, D. Ocher in prehistory: 300,000 years of the use of iron ores as pigments. In *Coming Age Iron*; Wertime, T.A., Muhly, J.D., Eds.; Yale University Press: New Haven, CT, USA, 1980.
48. Guglielmi, V.; Andreoli, M.; Comite, V.; Baroni, A.; Fermo, P. The combined use of SEM-EDX, Raman, ATR-FTIR and visible reflectance techniques for the characterisation of Roman wall painting pigments from Monte d'Oro area (Rome): An insight into red, yellow and pink shades. *Environ. Sci. Pollut. Res.* **2022**, *29*, 29419–29437. [CrossRef] [PubMed]

49. Magrini, D.; Bracci, S.; Bartolozzi, G.; Iannaccone, R.; Lenzi, S.; Liverani, P. Revealing Mithras' Color with the ICVBC Mobile Lab in the Museum. *Heritage* **2019**, *2*, 2160–2170. [CrossRef]
50. Grifa, C.; Cavassa, L.; De Bonis, A.; Germinario, C.; Guarino, V.; Izzo, F.; Kakoulli, I.; Langella, A.; Mercurio, M.; Morra, V. Beyond Vitruvius: New Insight in the Technology of Egyptian Blue and Green Frits. *J. Am. Ceram. Soc.* **2016**, *99*, 3467–3475. [CrossRef]
51. Kakoulli, I. *Greek Painting Techniques and Materials: From the Fourth to the First Century BC*; Archetype Book; University of Michigan: Ann Arbor, MI, USA, 2009.
52. Berke, H. The invention of blue and purple pigments in ancient times. *Chem. Soc. Rev.* **2006**, *36*, 15–30. [CrossRef] [PubMed]
53. Rodler, A.S.; Matthys, S.M.; Brons, C.; Artioli, G.; Snoeck, C.; Debaille, V.; Goderis, S. Investigating the provenance of Egyptian blue pigments in ancient Roman polychromy. *Archeometriai Műhely* **2021**, *18*, 97–108. [CrossRef]
54. Siddall, R. Mineral Pigments in Archaeology: Their Analysis and the Range of Available Materials. *Minerals* **2018**, *8*, 201. [CrossRef]
55. Mazzocchin, G.; Agnoli, F.; Colpo, I. Investigation of roman age pigments found on pottery fragments. *Anal. Chim. Acta* **2003**, *478*, 147–161. [CrossRef]
56. Anselmi, C.; Vagnini, M.; Seccaroni, C.; Azzarelli, M.; Frizzi, T.; Alberti, R.; Falcioni, M.; Sgamellotti, A. Imaging the antique: Unexpected Egyptian blue in Raphael's Galatea by non-invasive mapping. *Rend. Lince* **2020**, *31*, 913–917. [CrossRef]
57. Jaksch, H.; Seipel, W.; Weiner, K.L.; El Goresy, A. Egyptian blue? Cuprorivaite a window to ancient Egyptian technology. *Sci. Nat.* **1983**, *70*, 525–535. [CrossRef]
58. Eastaugh, N.; Walsh, V.; Chaplin, T.; Siddall, R. *Pigment Compendium: A Dictionary and Optical Microscopy of Historic Pigments*; Butterworth-Heinemann: London, UK, 2008.
59. Alberghina, M.F.; Germinario, C.; Bartolozzi, G.; Bracci, S.; Grifa, C.; Izzo, F.; La Russa, M.; Magrini, D.; Massa, E.; Mercurio, M.; et al. The Tomb of the Diver and the frescoed tombs in Paestum (southern Italy): New insights from a comparative archaeometric study. *PLoS ONE* **2020**, *15*, e0232375. [CrossRef] [PubMed]